УДК 539.3, 539.422.23, 531.011, 51-74, 519-62

ПОСТРОЕНИЕ МЕХАНИКО-МАТЕМАТИЧЕСКОЙ МОДЕЛИ ВЯЗКОУПРУГОГО БЛОЧНОГО ЭЛЕМЕНТА ДЛЯ РЕШЕНИЯ ДИНАМИЧЕСКИХ ЗАДАЧ ГЕОМЕХАНИКИ МЕТОДОМ ДИСКРЕТНЫХ ЭЛЕМЕНТОВ

М. А. НИКОЛАЙЧИК[1)]***, ЧЖАН ШИЦИ***[1)]

[1)]*Белорусский государственный университет, пр. Независимости, 4, 220030, г. Минск, Беларусь*

Аннотация. Рассматриваются методы численного моделирования, которые являются эффективными инструментами решения инженерно-геомеханических задач. Приводится процедура построения механико-математической модели одного типа вязкоупругого блочного элемента. На основе такого типа блочных элементов представляется возможным использование метода дискретных элементов для моделирования состояния массива горных пород в областях, где предположение о сплошности нарушается. Результирующие уравнения, описывающие поведение предложенного блочного элемента, получены с применением классических законов механики. Выполнен ряд численных экспериментов, рассмотрены различные варианты начальных условий, а также параметры связей между элементами блока. Разработан алгоритм, позволяющий описывать динамику блока, состоящего из n элементов. Проведена оценка быстродействия разработанного алгоритма с использованием

Образец цитирования:
Николайчик МА, Чжан Шици. Построение механико-математической модели вязкоупругого блочного элемента для решения динамических задач геомеханики методом дискретных элементов. *Журнал Белорусского государственного университета. Математика. Информатика.* 2024;3: 40–61 (на англ.).
EDN: GORQYA

For citation:
Nikolaitchik MA, Zhang Shiqi. Construction of mechanical and mathematical model of viscoelastic block element for solving geomechanics dynamic problems using discrete element method. *Journal of the Belarusian State University. Mathematics and Informatics.* 2024;3:40–61.
EDN: GORQYA

Авторы:
Михаил Александрович Николайчик – кандидат физико-математических наук; заведующий научно-исследовательской лабораторией прикладной механики механико-математического факультета.
Чжан Шици – магистрант кафедры теоретической и прикладной механики механико-математического факультета. Научный руководитель – М. А. Журавков.

Authors:
Mikhail A. Nikolaitchik, PhD (physics and mathematics); head of the laboratory of applied mechanics, faculty of mechanics and mathematics.
nikolaitchik.m@gmail.com
Zhang Shiqi, master's degree student at the department of theoretical and applied mechanics, faculty of mechanics and mathematics.
shiqizhang177@gmail.com

последовательных и параллельных вычислений. Полученные результаты могут применяться для решения динамических задач геомеханики методом дискретных элементов в областях породного массива, в которых нарушается гипотеза о сплошности.

Ключевые слова: численное моделирование; механико-математическое моделирование; механика деформируемого твердого тела; элементы дискретного метода; граничные условия; подземная геомеханика; деформируемый блочный элемент.

Благодарность. Исследование выполнено в рамках совместного проекта «Высокопроизводительный метод дискретных элементов для сыпучих материалов произвольной формы и его применение в геотехнике холодных регионов и горнодобывающих районов» Белорусского республиканского фонда фундаментальных исследований и Национального фонда естественных наук Китая.

CONSTRUCTION OF MECHANICAL AND MATHEMATICAL MODEL OF VISCOELASTIC BLOCK ELEMENT FOR SOLVING GEOMECHANICS DYNAMIC PROBLEMS USING DISCRETE ELEMENT METHOD

***M. A. NIKOLAITCHIK*[a], *ZHANG SHIQI*[a]**

[a]*Belarusian State University, 4 Niezaliezhnasci Avenue, Minsk 220030, Belarus*
Corresponding author: M. A. Nikolaitchik (nikolaitchik.m@gmail.com)

Abstract. Numerical simulation methods have become one of the effective tools to solve geomechanical engineering problems. The paper presents a procedure for constructing a mechanical and mathematical model of one type of viscoelastic block element. Based on this type of block element, it seems possible to apply the discrete element method for modelling the state of a rock massif in areas where the continuity assumption is violated. The resulting equations describing the behaviour of the proposed block element are obtained using classical laws of mechanics. A number of numerical experiments were carried out, different variants of initial conditions were considered, as well as parameters of connections between the elements of the block. An algorithm is developed to describe the block consisting of n elements dynamics. The performance of the developed algorithm using sequential and parallel computations has been evaluated. The obtained results can be used to solve dynamic problems of geomechanics by the discrete element method in the areas of rock massif where the continuity hypothesis is violated.

Keywords: numerical simulation; mechanic-mathematical modelling; mechanics of deformable solids; discrete method elements; boundary conditions; underground geomechanics; deformable block element.

Acknowledgements. This research was carried out as part of the joint project «High-performance discrete element method for granular materials of arbitrary shape and its application in geotechnics of cold regions and mining areas» of the Belarusian Republican Foundation for Fundamental Research and the National Natural Science Foundation of China.

Introduction

Currently, combined continuous and discrete models are increasingly used when solving subsurface geomechanical problems. In 1996, researcher T. Belytschko from the Northwestern University in the United States proposed a meshless approximation based on moving least-squares, kernels, and partitions of unity [1]. Then in 2004, S. H. Li and others from Asia proposed a continuum-based discrete element method for a continuous deformation and failure process [2]. And just after two years, in 2006, A. K. Ariffin and his colleagues used the numerical modelling based on the combination of finite element method (FEM) and the discrete element method (DEM) to simulate crack propagation under mixed mode loading [3]. In 2008, A. Karami and D. Stead investigates the processes of joint surface damage and near-surface intact rock tensile failure using a hybrid FEM and DEM code [4]. Also J. P. Morris and other researchers investigated the effect of explosive and impact loading on geological media using the FEM and DEM methods [5]. In 2022, D. S. Zhurkina and her colleagues simulated the modelling of shear localisation and transition of the geoenvironment to unstable deformation modes based on the DEM [6]. In addition, many scientists have analysed the application of numerical methods in geomechanics[1].

[1]*Zhuravkov M. A.* Modern numerical methods in mechanics : a course of lectures. Minsk : Belarus. State Univ., 2022. 132 p.

Continuous numerical methods (FEM, boundary element method (BEM)) are used when studying the stress-strain state (SSS) in regions distant from the underground rock mass structure [7]. Continuum methods [8] are not completely suitable for considering regions of rock masses with clearly identified block structures or fracture zones, whereas discrete methods allow the disruption of the continuity hypothesis to be of great help in studying rocks. And when studying the behaviour of nearby regions, it is more suitable and accurately to use the DEM for modelling with various modifications, which makes it possible to directly consider cracks and block structures [9].

Let us consider the modelling problem of constructing general models that allow us to study deformation processes and rock mass states in the regions where massive structures are formed. For the rock mass, its initial state can be considered within the framework of continuum mechanics, while its structure cannot be ignored when studying the SSS of rock mass when it is in an obviously massive region.

According to the simplified definition of regular packing [10], its parameters can be determined experimentally rather than theoretically, by calibrating the model using field measurement data from real rock masses in the structural state under study.

Therefore, we imagine discontinuous regions of a rock mass as regular accumulations of blocks. In the DEM, deformations in the block structure are considered to be due only to the connections between individual elements [11].

Let us consider the following approach to study the deformation of individual blocks, representing the block as a system consisting of multiple internal solid elements interconnected by several connections (fig. 1).

Therefore, the deformation of the block occurs due to the deformation of the connections between elements, which are considered as solid bodies. In this case, the entire discontinuous area is a system of several such block elements, which in turn are connected to each other by certain connections. That is, in order to simulate damaged or fractured areas in a rock mass, such block elements should be placed over all discontinuous areas.

We introduce the following restrictions on the shape of the individual elements in the overall block structure. The shape of the elements is symmetrical. Additionally, elements can have various shapes and sizes. We impose the same restriction on the connections between elements: in the general structure, the connections of the element i to its neighbours are symmetrical.

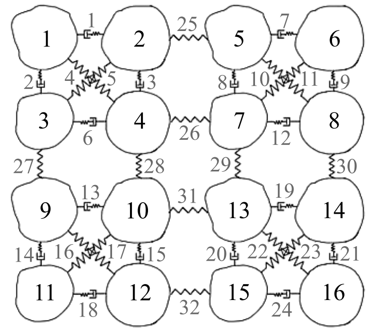

Fig. 1. The model of blocks consisting of 16 elements

Therefore, the following problem is considered as a basic modelling problem: the study of the state of a planar structure consisting of internal elements which are interconnected by elastic and viscous connections when subjected to external loads (see fig. 1).

Construction of basic models

Let us consider the following model problem. As mentioned before, the state of the block shown in the previous fig. 1 is studied in the case of $m_i = m$, $i = \overline{1, 16}$. That is, the mass of each element is m, and the distance between the centroids of the internal components is l. Elements are connected by elastic and viscous damping links: $l_4, l_5, l_{10}, l_{11}, l_{16}, l_{17}, l_{22}, l_{23}, l_{25}, l_{26}, l_{27}, l_{28}, l_{29}, l_{30}, l_{31}, l_{32}$ are elastic connections with stiffness coefficient k; $l_1, l_2, l_3, l_6, l_7, l_8, l_9, l_{12}, l_{13}, l_{14}, l_{15}, l_{18}, l_{19}, l_{20}, l_{21}, l_{24}$ are viscous links with a damping coefficient c. Each element m_i in the system is displaced x_i in the horizontal X-axis direction by a certain amount due to the overall (see fig. 1).

We solve the problem analytically using the Lagrangian equations of the second kind[2]. In order to consider the damping, it is necessary to introduce additional terms in the right part of the Lagrangian equations, taking into account the presence of medium resistance. Let the damping coefficient be η. Let us define a dissipation function G such that the resistance of the medium f and the dissipation function G satisfy the following relationship[3]:

$$f = -\frac{\partial G}{\partial \dot{x}}. \quad (1)$$

It can be seen from the appearance of (1) that the dissipation function G has a power dimension, which itself reflects the loss rate of mechanical energy [12]. Taking into account the assumptions introduced, the Lagrangian equations of the second kind can be written as follows:

[2]*Vyarvilskaya O. N., Medvedev D. G., Savchuk V. P.* A short course in theoretical mechanics : textbook. Minsk : Belarus. State Univ., 2020. 207 p.

[3]*Shakirzyanov R. A., Shakirzyanov F. R.* Dynamics and stability of structures : textbook. 2nd ed., revised. Kazan : Publ. House of the Kazan State Univ. of Archit. and Eng., 2015. 120 p.

$$\frac{d}{dt}\frac{\partial L}{\partial \dot{x}_i} - \frac{\partial L}{\partial x_i} = -\frac{\partial G}{\partial \dot{x}_i},\ i = \overline{1, 16}. \tag{2}$$

For calculating, it is easier to divide the entire system into four parts, the first part contains elements 1, 2, 3, 4 (fig. 2). Calculate the Lagrangian equation for the first part.

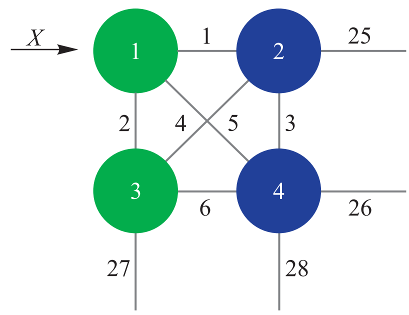

Fig. 2. The first part of model consisting of 16 elements

The kinetic energy (3) for this part is

$$T = \sum_{i=1}^{4} T_i = \frac{1}{2}m\dot{x}_1^2 + \frac{1}{2}m\dot{x}_2^2 + \frac{1}{2}m\dot{x}_3^2 + \frac{1}{2}m\dot{x}_4^2. \tag{3}$$

The potential energy (4) of the system is

$$\Pi = \sum_{j=1}^{6} \frac{k}{2}\Delta l_j^2. \tag{4}$$

It is determined by the potential energy of elastic connections (springs). From geometric considerations for the first part, the spring displacements (5) are equal to

$$\begin{gathered}
\Delta l_1 = (x_1 + x_2), \\
\Delta l_2 = \sqrt{l^2 + (x_1 - x_3)^2} - l, \\
\Delta l_3 = \sqrt{l^2 + (x_2 - x_4)^2} - l, \\
\Delta l_4 = \sqrt{l^2 + (l - x_1 - x_4)^2} - l, \\
\Delta l_5 = \sqrt{l^2 + (l - x_2 - x_3)^2} - l, \\
\Delta l_6 = (x_3 + x_4), \\
\Delta l_{25} = (x_2 + x_5), \\
\Delta l_{26} = (x_4 + x_7), \\
\Delta l_{27} = \sqrt{l^2 + (x_3 - x_9)^2} - l, \\
\Delta l_{28} = \sqrt{l^2 + (x_4 - x_{10})^2} - l.
\end{gathered} \tag{5}$$

Then, the expression for potential energy takes the form defined by formula (6):

$$\begin{aligned}
\Pi = \frac{k}{2}\Bigg(& (x_1 + x_2)^2 + \left(\sqrt{l^2 + (x_1 - x_3)^2} - l\right)^2 + \left(\sqrt{l^2 + (l - x_2 - x_3)^2} - l\right)^2 + \\
& + \left(\sqrt{l^2 + (x_2 - x_4)^2} - l\right)^2 + \left(\sqrt{l^2 + (l - x_1 - x_4)^2} - l\right)^2 + \\
& + (x_3 + x_4)^2 + (x_2 + x_5)^2 + (x_4 + x_7)^2 + \left(\sqrt{l^2 + (x_3 - x_9)^2} - l\right)^2 + \left(\sqrt{l^2 + (l - x_4 - x_{10})^2} - l\right)^2\Bigg).
\end{aligned} \tag{6}$$

As a result, the Lagrange function (7) is written as follows:

$$L = \frac{1}{2} m \left(x_1^2 + x_2^2 + x_3^2 + x_4^2 \right) - \frac{k}{2} \left(\left(x_1 + x_2 \right)^2 + \left(\sqrt{l^2 + \left(x_1 - x_3 \right)^2} - l \right)^2 + \right.$$
$$+ \left(\sqrt{l^2 + \left(l - x_2 - x_3 \right)^2} - l \right)^2 + \left(\sqrt{l^2 + \left(x_2 - x_4 \right)^2} - l \right)^2 + \left(\sqrt{l^2 + \left(l - x_1 - x_4 \right)^2} - l \right)^2 +$$
$$\left. + \left(x_3 + x_4 \right)^2 + \left(x_2 + x_5 \right)^2 + \left(x_4 + x_7 \right)^2 + \left(\sqrt{l^2 + \left(x_3 - x_9 \right)^2} - l \right)^2 + \left(\sqrt{l^2 + \left(l - x_4 - x_{10} \right)^2} - l \right)^2 \right). \quad (7)$$

For the dissipation function G (8) it takes form as

$$G = \sum_{j=1}^{6} \frac{\eta}{2} \Delta \dot{l}_j^2. \quad (8)$$

Where only vicious connections (damper) are considered, the geometric considerations for the first part, the damper displacements (9) are equal to

$$\begin{aligned} \Delta \dot{l}_1 &= \left(\dot{x}_1 + \dot{x}_2 \right), \\ \Delta \dot{l}_2 &= \frac{\left(x_1 - x_3 \right)\left(\dot{x}_1 - \dot{x}_3 \right)}{\sqrt{l^2 + \left(x_1 - x_3 \right)^2}}, \\ \Delta \dot{l}_3 &= \frac{\left(x_2 - x_4 \right)\left(\dot{x}_1 - \dot{x}_4 \right)}{\sqrt{l^2 + \left(x_2 - x_4 \right)^2}}, \\ \Delta \dot{l}_6 &= \left(\dot{x}_3 + \dot{x}_4 \right). \end{aligned} \quad (9)$$

Then the equation of the dissipation function G (10) is

$$G = \frac{\eta}{2} \left(\left(\dot{x}_1 + \dot{x}_2 \right)^2 + \left(\frac{\left(x_1 - x_3 \right)\left(\dot{x}_1 - \dot{x}_3 \right)}{\sqrt{l^2 + \left(x_1 - x_3 \right)^2}} \right)^2 + \left(\frac{\left(x_2 - x_4 \right)\left(\dot{x}_2 - \dot{x}_4 \right)}{\sqrt{l^2 + \left(x_2 - x_4 \right)^2}} \right)^2 + \left(\dot{x}_3 + \dot{x}_4 \right)^2 \right). \quad (10)$$

As a result, equations (2) for the first part where $i = 1, 2, 3, 4$ are written explicitly (11) as follows:

$$m\ddot{x}_1 + k \left(\left(x_1 + x_2 \right) + \left(\left(l^2 + \left(x_1 - x_3 \right)^2 \right)^{\frac{1}{2}} - l \right) \left(l^2 + \left(x_1 - x_3 \right)^2 \right)^{-\frac{1}{2}} \left(x_1 - x_3 \right) - \right.$$
$$\left. - \left(\left(l^2 + \left(l - x_1 - x_4 \right)^2 \right)^{\frac{1}{2}} - l \right) \left(l^2 + \left(l - x_1 - x_4 \right)^2 \right)^{-\frac{1}{2}} \left(l - x_1 - x_4 \right) \right) =$$
$$= -\eta \left(\left(\dot{x}_1 + \dot{x}_2 \right) + \frac{\left(x_1 - x_3 \right)^2 \left(\dot{x}_1 - \dot{x}_3 \right)}{l^2 + \left(x_1 - x_3 \right)^2} \right),$$

$$m\ddot{x}_2 + k \left(\left(x_1 + x_2 \right) + \left(\left(l^2 + \left(x_2 - x_4 \right)^2 \right)^{\frac{1}{2}} - l \right) \left(l^2 + \left(x_2 - x_4 \right)^2 \right)^{-\frac{1}{2}} \left(x_2 - x_4 \right) - \right.$$
$$\left. - \left(\left(l^2 + \left(l - x_2 - x_3 \right)^2 \right)^{\frac{1}{2}} - l \right) \left(l^2 + \left(l - x_2 - x_3 \right)^2 \right)^{-\frac{1}{2}} \left(l - x_2 - x_3 \right) + \left(x_2 + x_5 \right) \right) =$$
$$= -\eta \left(\left(\dot{x}_1 + \dot{x}_2 \right) + \frac{\left(x_2 - x_4 \right)^2 \left(\dot{x}_2 - \dot{x}_4 \right)}{l^2 + \left(x_2 - x_4 \right)^2} \right),$$

$$
\begin{aligned}
& m\ddot{x}_3 + k\Bigg((x_3 + x_4) - \left(\left(l^2 + (x_1 - x_3)^2\right)^{\frac{1}{2}} - l \right)\left(l^2 + (x_1 - x_3)^2\right)^{-\frac{1}{2}}(x_1 - x_3) + \\
& + \left(\left(l^2 + (x_3 - x_9)^2\right)^{\frac{1}{2}} - l \right)\left(l^2 + (x_3 - x_9)^2\right)^{-\frac{1}{2}}(x_3 - x_9) - \\
& - \left(\left(l^2 + (l - x_2 - x_3)^2\right)^{\frac{1}{2}} - l \right)\left(l^2 + (l - x_2 - x_3)^2\right)^{-\frac{1}{2}}(l - x_2 - x_3) \Bigg) = \\
& = -\eta\left((\dot{x}_3 + \dot{x}_4) - \frac{(x_1 - x_3)^2 (\dot{x}_1 - \dot{x}_3)}{l^2 + (x_1 - x_3)^2} \right), \\
& m\ddot{x}_4 + k\Bigg((x_3 + x_4) - \left(\left(l^2 + (x_2 - x_4)^2\right)^{\frac{1}{2}} - l \right)\left(l^2 + (x_2 - x_4)^2\right)^{-\frac{1}{2}}(x_2 - x_4) + \\
& + \left(\left(l^2 + (x_4 - x_{10})^2\right)^{\frac{1}{2}} - l \right)\left(l^2 + (x_4 - x_{10})^2\right)^{-\frac{1}{2}}(x_4 - x_{10}) - \\
& - \left(\left(l^2 + (l - x_1 - x_4)^2\right)^{\frac{1}{2}} - l \right)\left(l^2 + (l - x_1 - x_4)^2\right)^{-\frac{1}{2}}(l - x_1 - x_4) + (x_4 + x_7) \Bigg) = \\
& = -\eta\left((\dot{x}_3 + \dot{x}_4) - \frac{(x_2 - x_4)^2 (\dot{x}_2 - \dot{x}_4)}{l^2 + (x_2 - x_4)^2} \right).
\end{aligned}
\tag{11}
$$

For the remaining three parts ($i = \overline{5, 8}$, $i = \overline{9, 12}$, $i = \overline{13, 16}$), the same analysis method will be constructed. The second part contains elements 5, 6, 7, 8 (fig. 3).

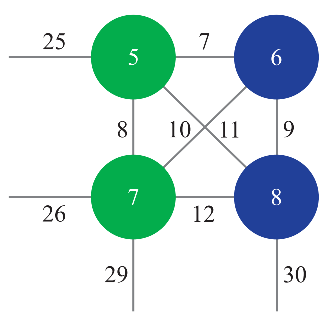

Fig. 3. The second part of model consisting of 16 elements

Equations (2) for the second part where $i = 5, 6, 7, 8$ are written explicitly (12) as follows:

$$
\begin{aligned}
& m\ddot{x}_5 + k\Bigg((x_5 + x_6) + \left(\left(l^2 + (x_5 - x_7)^2\right)^{\frac{1}{2}} - l \right)\left(l^2 + (x_5 - x_7)^2\right)^{-\frac{1}{2}}(x_5 - x_7) - \\
& - \left(\left(l^2 + (l - x_5 - x_8)^2\right)^{\frac{1}{2}} - l \right)\left(l^2 + (l - x_5 - x_8)^2\right)^{-\frac{1}{2}}(l - x_5 - x_8) + (x_2 + x_5) \Bigg) = \\
& = -\eta\left((\dot{x}_5 + \dot{x}_6) + \frac{(x_5 - x_7)^2 (\dot{x}_5 - \dot{x}_7)}{l^2 + (x_5 - x_7)^2} \right),
\end{aligned}
$$

$$
\begin{gathered}
m\ddot{x}_6 + k\left((x_5 + x_6) + \left(\left(l^2 + (x_6 - x_8)^2 \right)^{\frac{1}{2}} - l \right) \left(l^2 + (x_6 - x_8)^2 \right)^{-\frac{1}{2}} (x_6 - x_8) - \right. \\
\left. - \left(\left(l^2 + (l - x_6 - x_7)^2 \right)^{\frac{1}{2}} - l \right) \left(l^2 + (l - x_6 - x_7)^2 \right)^{-\frac{1}{2}} (l - x_6 - x_7) \right) = \\
= -\eta \left((\dot{x}_5 + \dot{x}_6) + \frac{(x_6 - x_8)^2 (\dot{x}_6 - \dot{x}_8)}{l^2 + (x_6 - x_8)^2} \right), \\
m\ddot{x}_7 + k\left((x_7 + x_8) - \left(\left(l^2 + (x_5 - x_7)^2 \right)^{\frac{1}{2}} - l \right) \left(l^2 + (x_5 - x_7)^2 \right)^{-\frac{1}{2}} (x_5 - x_7) + \right. \\
+ \left(\left(l^2 + (x_7 - x_{13})^2 \right)^{\frac{1}{2}} - l \right) \left(l^2 + (x_7 - x_{13})^2 \right)^{-\frac{1}{2}} (x_7 - x_{13}) - \\
\left. - \left(\left(l^2 + (l - x_6 - x_7)^2 \right)^{\frac{1}{2}} - l \right) \left(l^2 + (l - x_6 - x_7)^2 \right)^{-\frac{1}{2}} (l - x_6 - x_7) + (x_4 + x_7) \right) = \\
= -\eta \left((\dot{x}_7 + \dot{x}_8) - \frac{(x_5 - x_7)^2 (\dot{x}_5 - \dot{x}_7)}{l^2 + (x_5 - x_7)^2} \right), \\
m\ddot{x}_8 + k\left((x_7 + x_8) - \left(\left(l^2 + (x_6 - x_8)^2 \right)^{\frac{1}{2}} - l \right) \left(l^2 + (x_6 - x_8)^2 \right)^{-\frac{1}{2}} (x_6 - x_8) + \right. \\
+ \left(\left(l^2 + (x_8 - x_{14})^2 \right)^{\frac{1}{2}} - l \right) \left(l^2 + (x_8 - x_{14})^2 \right)^{-\frac{1}{2}} (x_8 - x_{14}) - \\
\left. - \left(\left(l^2 + (l - x_5 - x_8)^2 \right)^{\frac{1}{2}} - l \right) \left(l^2 + (l - x_5 - x_8)^2 \right)^{-\frac{1}{2}} (l - x_5 - x_8) \right) = \\
= -\eta \left((\dot{x}_7 + \dot{x}_8) - \frac{(x_6 - x_8)^2 (\dot{x}_6 - \dot{x}_8)}{l^2 + (x_6 - x_8)^2} \right).
\end{gathered}
\tag{12}
$$

The third part contains elements 9, 10, 11, 12 (fig. 4):

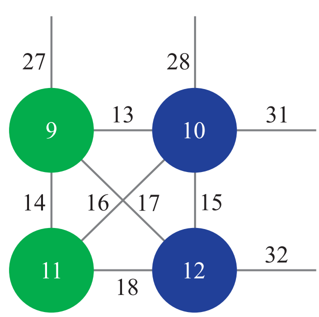

Fig. 4. The third part of model consisting of 16 elements

Equations (2) for the third part where $i = 9, 10, 11, 12$ are written explicitly (13) as follows:

$$
\begin{gathered}
m\ddot{x}_9 + k\left((x_9 + x_{10}) + \left(\left(l^2 + (x_9 - x_{11})^2\right)^{\frac{1}{2}} - l \right)\left(l^2 + (x_9 - x_{11})^2\right)^{-\frac{1}{2}}(x_9 - x_{11}) - \right. \\
- \left(\left(l^2 + (x_3 - x_9)^2\right)^{\frac{1}{2}} - l \right)\left(l^2 + (x_3 - x_9)^2\right)^{-\frac{1}{2}}(x_3 - x_9) - \\
\left. - \left(\left(l^2 + (l - x_9 - x_{12})^2\right)^{\frac{1}{2}} - l \right)\left(l^2 + (l - x_9 - x_{12})^2\right)^{-\frac{1}{2}}(l - x_9 - x_{12}) \right) = \\
= -\eta\left((\dot{x}_9 + \dot{x}_{10}) + \frac{(x_9 - x_{11})^2 (\dot{x}_9 - \dot{x}_{11})}{l^2 + (x_9 - x_{11})^2} \right), \\
m\ddot{x}_{10} + k\left((x_9 + x_{10}) + \left(\left(l^2 + (x_{10} - x_{12})^2\right)^{\frac{1}{2}} - l \right)\left(l^2 + (x_{10} - x_{12})^2\right)^{-\frac{1}{2}}(x_{10} - x_{12}) - \right. \\
- \left(\left(l^2 + (x_4 - x_{10})^2\right)^{\frac{1}{2}} - l \right)\left(l^2 + (x_4 - x_{10})^2\right)^{-\frac{1}{2}}(x_4 - x_{10}) - \\
\left. - \left(\left(l^2 + (l - x_{10} - x_{11})^2\right)^{\frac{1}{2}} - l \right)\left(l^2 + (l - x_{10} - x_{11})^2\right)^{-\frac{1}{2}}(l - x_{10} - x_{11}) + (x_{10} + x_{13}) \right) = \\
= -\eta\left((\dot{x}_9 + \dot{x}_{10}) + \frac{(x_{10} - x_{12})^2 (\dot{x}_{10} - \dot{x}_{12})}{l^2 + (x_{10} - x_{12})^2} \right), \\
m\ddot{x}_{11} + k\left((x_{11} + x_{12}) - \left(\left(l^2 + (x_9 - x_{11})^2\right)^{\frac{1}{2}} - l \right)\left(l^2 + (x_9 - x_{11})^2\right)^{-\frac{1}{2}}(x_9 - x_{11}) - \right. \\
\left. - \left(\left(l^2 + (l - x_{10} - x_{11})^2\right)^{\frac{1}{2}} - l \right)\left(l^2 + (l - x_{10} - x_{11})^2\right)^{-\frac{1}{2}}(l - x_{10} - x_{11}) \right) = \\
= -\eta\left((\dot{x}_{11} + \dot{x}_{12}) - \frac{(x_9 - x_{11})^2 (\dot{x}_9 - \dot{x}_{11})}{l^2 + (x_9 - x_{11})^2} \right), \\
m\ddot{x}_{12} + k\left((x_{11} + x_{12}) - \left(\left(l^2 + (x_{10} - x_{12})^2\right)^{\frac{1}{2}} - l \right)\left(l^2 + (x_{10} - x_{12})^2\right)^{-\frac{1}{2}}(x_{10} - x_{12}) - \right. \\
\left. - \left(\left(l^2 + (l - x_9 - x_{12})^2\right)^{\frac{1}{2}} - l \right)\left(l^2 + (l - x_9 - x_{12})^2\right)^{-\frac{1}{2}}(l - x_9 - x_{12}) + (x_{12} + x_{15}) \right) = \\
= -\eta\left((\dot{x}_{11} + \dot{x}_{12}) - \frac{(x_{10} - x_{12})^2 (\dot{x}_{10} - \dot{x}_{12})}{l^2 + (x_{10} - x_{12})^2} \right).
\end{gathered}
\tag{13}
$$

The fourth part contains elements 13, 14, 15, 16 (fig. 5):

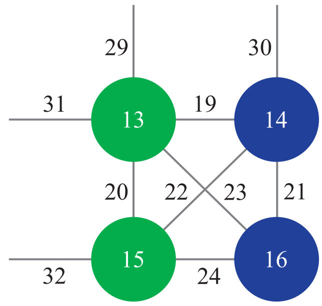

Fig. 5. The fourth part of model consisting of 16 elements

Equations (2) for the fourth part where $i = 13, 14, 15, 16$ are written explicitly (14) as follows:

$$m\ddot{x}_{13} + k\Bigg((x_{13} + x_{14}) + \left(\left(l^2 + (x_{13} - x_{15})^2\right)^{\frac{1}{2}} - l\right)\left(l^2 + (x_{13} - x_{15})^2\right)^{-\frac{1}{2}}(x_{13} - x_{15}) -$$

$$- \left(\left(l^2 + (x_7 - x_{13})^2\right)^{\frac{1}{2}} - l\right)\left(l^2 + (x_7 - x_{13})^2\right)^{-\frac{1}{2}}(x_7 - x_{13}) -$$

$$- \left(\left(l^2 + (l - x_{13} - x_{16})^2\right)^{\frac{1}{2}} - l\right)\left(l^2 + (l - x_{13} - x_{16})^2\right)^{-\frac{1}{2}}(l - x_{13} - x_{16}) + (x_{10} + x_{13})\Bigg) =$$

$$= -\eta\left((\dot{x}_{13} + \dot{x}_{14}) + \frac{(x_{13} - x_{15})^2(\dot{x}_{13} - \dot{x}_{15})}{l^2 + (x_{13} - x_{15})^2}\right),$$

$$m\ddot{x}_{14} + k\Bigg((x_{13} + x_{14}) + \left(\left(l^2 + (x_{14} - x_{16})^2\right)^{\frac{1}{2}} - l\right)\left(l^2 + (x_{14} - x_{16})^2\right)^{-\frac{1}{2}}(x_{14} - x_{16}) -$$

$$- \left(\left(l^2 + (x_8 - x_{14})^2\right)^{\frac{1}{2}} - l\right)\left(l^2 + (x_8 - x_{14})^2\right)^{-\frac{1}{2}}(x_8 - x_{14}) -$$

$$- \left(\left(l^2 + (l - x_{14} - x_{15})^2\right)^{\frac{1}{2}} - l\right)\left(l^2 + (l - x_{14} - x_{15})^2\right)^{-\frac{1}{2}}(l - x_{14} - x_{15})\Bigg) =$$

$$= -\eta\left((\dot{x}_{13} + \dot{x}_{14}) + \frac{(x_{14} - x_{16})^2(\dot{x}_{14} - \dot{x}_{16})}{l^2 + (x_{14} - x_{16})^2}\right),$$

$$m\ddot{x}_{15} + k\Bigg((x_{15} + x_{16}) - \left(\left(l^2 + (x_{13} - x_{15})^2\right)^{\frac{1}{2}} - l\right)\left(l^2 + (x_{13} - x_{15})^2\right)^{-\frac{1}{2}}(x_{13} - x_{15}) -$$

$$- \left(\left(l^2 + (l - x_{14} - x_{15})^2\right)^{\frac{1}{2}} - l\right)\left(l^2 + (l - x_{14} - x_{15})^2\right)^{-\frac{1}{2}}(l - x_{14} - x_{15}) + (x_{15} + x_{16})\Bigg) =$$

$$= -\eta\left((\dot{x}_{15} + \dot{x}_{16}) - \frac{(x_{13} - x_{15})^2(\dot{x}_{13} - \dot{x}_{15})}{l^2 + (x_{13} - x_{15})^2}\right),$$

$$m\ddot{x}_{16}+k\left(\left(x_{15}+x_{16}\right)-\left(\left(l^2+\left(x_{14}-x_{16}\right)^2\right)^{\frac{1}{2}}-l\right)\left(l^2+\left(x_{14}-x_{16}\right)^2\right)^{-\frac{1}{2}}\left(x_{14}-x_{16}\right)-\right.$$
$$\left.-\left(\left(l^2+\left(l-x_{13}-x_{16}\right)^2\right)^{\frac{1}{2}}-l\right)\left(l^2+\left(l-x_{13}-x_{16}\right)^2\right)^{-\frac{1}{2}}\left(l-x_{13}-x_{16}\right)\right)= \qquad (14)$$
$$=-\eta\left(\left(\dot{x}_{15}+\dot{x}_{16}\right)-\frac{\left(x_{14}-x_{16}\right)^2\left(\dot{x}_{14}-\dot{x}_{16}\right)}{l^2+\left(x_{14}-x_{16}\right)^2}\right).$$

In order to solve this set of differential equations about time, we choose the NDSolve method in computer software *Wolfram Mathematica* [13].

When computing NDSolve, there are usually three stages. Firstly, the given system of equations is converted into a function that represents the terms on the right-hand side of the system of equations in the normal form. Secondly, it is solved iteratively starting from the initial conditions. Thirdly, the data stored during the iterative process is processed into one or more InterpolatingFunction objects. Using the functions in NDSolve, one can have more control over the iterative process. These steps are tied together by an NDSolve StateData object, which can retain all the solved differentials.

In order to get a specific solution, we also need to enter the initial boundary conditions in the NDSolve code. So now we will consider various variants for different initial conditions for the introduced block model.

Under the initial displacement. The parameters and the initial conditions are

$$m = 2\text{ kg},\ l = 0.1\text{ m},\ k = 100\text{ N/m},\ c = 0.5\text{ N}\cdot\text{s/m},\ t = 10\text{ s}.$$

There is an initial displacement in the horizontal direction to any element which is shown below (fig. 6), and in this variant the value is $x_1 = 0.05$ m.

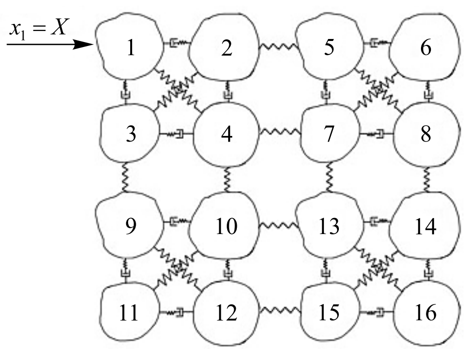

Fig. 6. The initial displacement

And the following pictures (fig. 7) show the motion of the system in the first 10 s under the initial displacement conditions.

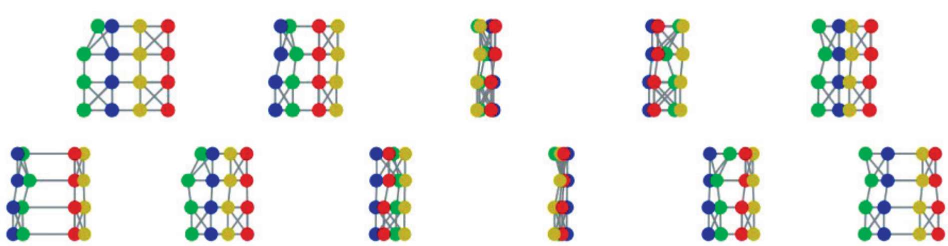

Fig. 7. The motion of model in 0–10 s under initial displacement

Under the initial velocity. The parameters and the initial conditions are

$$m = 2\text{ kg},\ l = 0.1\text{ m},\ k = 100\text{ N/m},\ c = 0.5\text{ N}\cdot\text{s/m},\ t = 10\text{ s}.$$

There is an initial velocity in the horizontal direction to any element which is shown below (fig. 8), and in this variant the value is $v_1 = 0.5$ m/s.

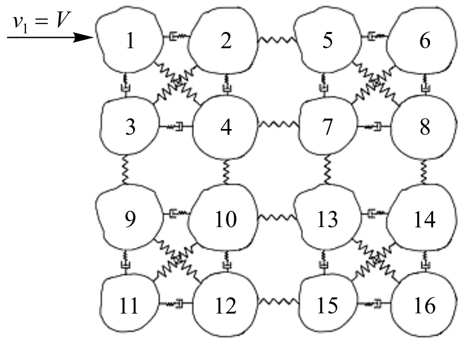

Fig. 8. The initial velocity

And the following pictures (fig. 9) show the motion of the system in the first 10 s under the initial velocity conditions.

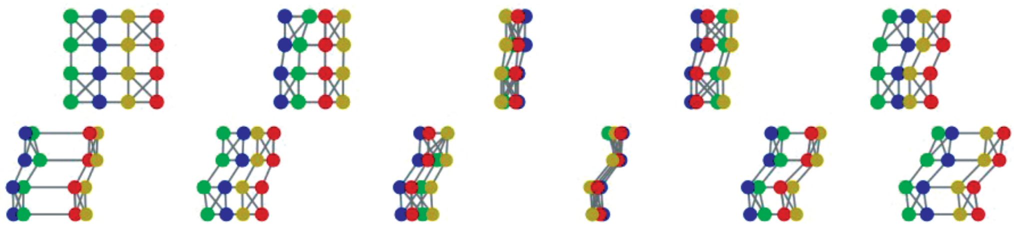

Fig. 9. The motion of model in 0–10 s under initial velocity

Under the initial impulse. The parameters and the initial conditions are

$$m = 2 \text{ kg}, \ l = 0.1 \text{ m}, \ k = 100 \text{ N/m}, \ c = 0.5 \text{ N} \cdot \text{s/m}, \ t = 10 \text{ s}.$$

There is an initial impulse in the horizontal direction to any element which is shown below (fig. 10), and the initial impulse with the function (15) in this variant (fig. 11) is

$$F(t) = P\left(tH(t) - 2\left(t - \frac{1}{2}\right)H\left(t - \frac{1}{2}\right) + (t-1)H(t-1)\right), \tag{15}$$

where H is the Heaviside function[4].

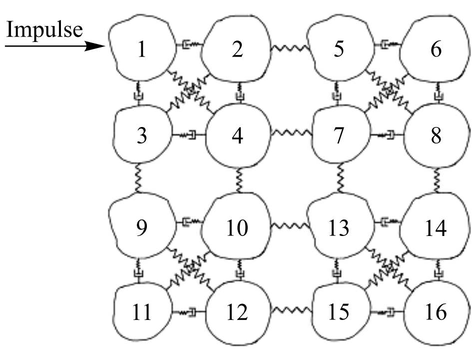

Fig. 10. The initial impulse

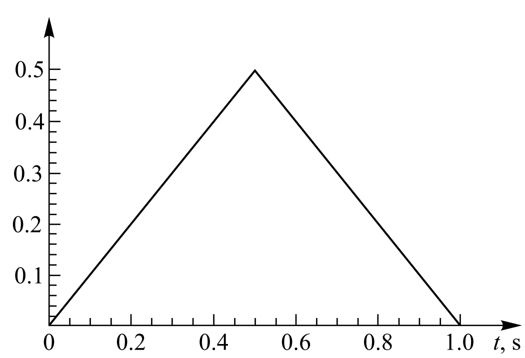

Fig. 11. Dynamic load in the form of a triangular impulse

The variant can be solved by using the momentum theorem written as formula (16):

$$F(t)\Delta t = m(v_1 - v_0). \tag{16}$$

And the initial velocity of system is 0, so compute the velocity (17) at $t = 1$ s:

$$v_1 = \frac{F(t)\Delta t + mv_0}{m} = \frac{\int_0^{t_*} F(\tau)d\tau}{m}. \tag{17}$$

[4]*Evseev N. A.* Elements of harmonic analysis. Novosibirsk : Novosibirsk State Univ., 2017. 97 p.

Then the same impulse condition is translated to the condition when $t = 1$ s, the velocity of the element 1 is v_1. In this variant $v_{1(t=1)} = 0.125$ m/s. And the following picture (fig. 12) shows the motion of the system in the first 10 s under the initial impulse condition.

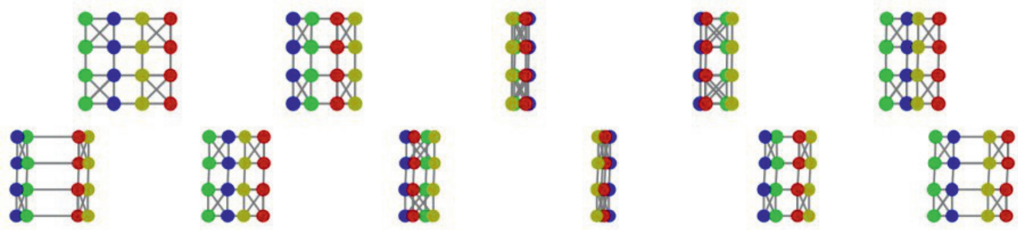

Fig. 12. The motion of model in 0–10 s under initial impulse

Under the different elastic coefficients. Different elastic coefficients will change the motion state of the model [14]. For the same initial conditions and parameters $m = 2$ kg, $l = 0.1$ m, $c = 0.5$ N · s/m, $t = 10$ s.

Let us study the difference between the elastic coefficient decreasing by 10 times ($k = 10$ N/m) and increasing by 10 times ($k = 1000$ N/m) under the same initial displacement conditions described in subdivision «Under the initial displacement» where $x_1 = 0.05$ m (fig. 13).

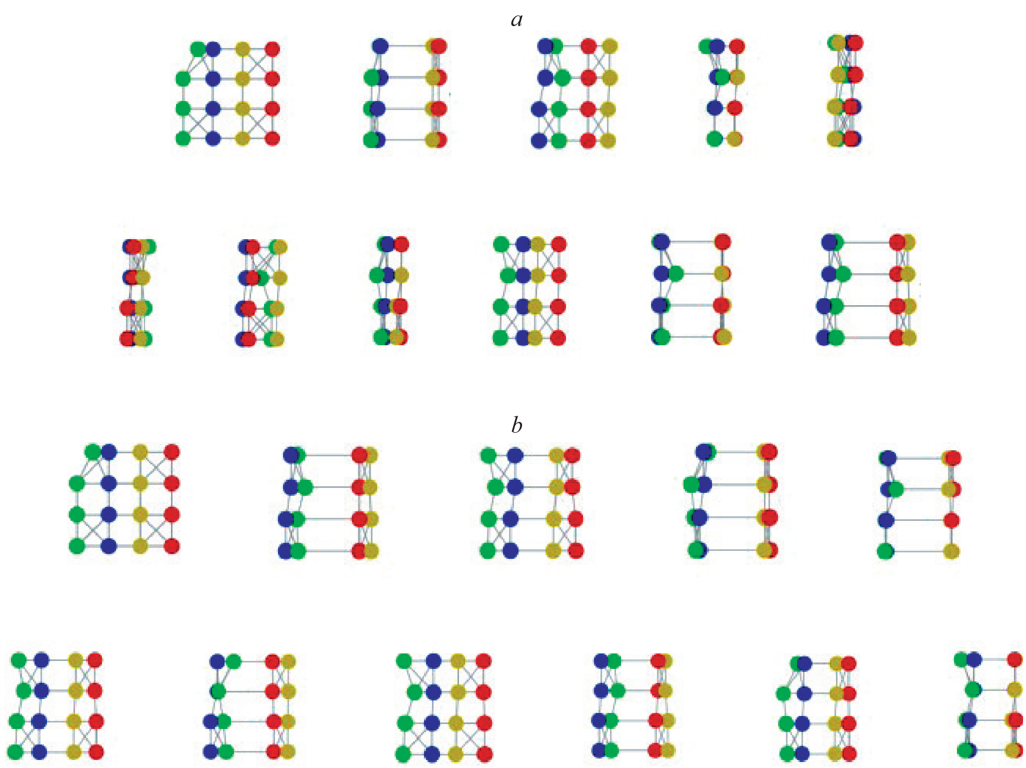

Fig. 13. The motion of the model in 0–10 s under the different elastic coefficients: $k = 10$ N/m (*a*); $k = 1000$ N/m (*b*)

Implementation of parallel computing in the *Wolfram Mathematica* system

The *Wolfram Mathematica's* computer algebra system is a very efficient means of calculation. Today the system contains about 5000 functions, many of which were originally written in an optimised form (especially for low-level calculations). Most computational functions in *Wolfram Mathematica*, such as dimensionality reduction operations, statistical data processing, processing images and other are widely used. However, there is a set of tools (such as ParallelSum, Parallelise, ParallelMap, ParallelTable, ParallelArray, ParallelCombine, etc.) that can significantly speed up code calculations when implementing multi-threaded tasks [15].

Let us take the previous task as an example. We used NDSolve for sequential calculation before. The calculation rule is time iteration, and the AbsoluteTiming function outputs the final calculation result in seconds.

The calculation time is as follows. Of course, it should be emphasised that all computer calculations in this paper were performed based on the following configuration: Intel(R) Core(TM) i5-9300-H CPU / NVIDIA GeForce GTX 1650. The absolute time of the sequential calculation for the code is $T_1 = 0.988\,049$ s.

Parallel computing refers to the process of using multiple computing resources to solve computing problems at the same time. It is an effective means to improve the computing speed and processing the power of computer systems [16]. Its basic idea is to use multiple processors to collaboratively solve the same problem, that is, to decompose the problem to be solved into several parts, and each part is calculated in parallel by an independent processor. A parallel computing system can be either a specially designed supercomputer containing multiple processors or a cluster of several independent computers interconnected in some way. Data processing is completed through parallel computing clusters, and the processing results are returned to the user.

Different from NDSolve, ParallelEvaluate performs parallel calculations on differential equations, which greatly shortens the calculation time while achieving the same calculation purpose.

Under the same configuration environment, the absolute time of parallel calculation is $T_p = 0.176\,067$ s.

In order to measure the effect of parallel computing, we introduce two parameters: acceleration and efficiency.

The formula of acceleration (18) is

$$S_p = \frac{T_1}{T_p}, \tag{18}$$

where p refers to the number of central processing units, which in the paper is $p = 2$; T_1 refers to the execution time of the sequential execution algorithm; T_p refers to the execution time of a parallel algorithm when there are p processors.

The formula of efficiency (19) is

$$E_p = \frac{S_p}{p}. \tag{19}$$

When $S_p = p$, it can be called linear acceleration. When the acceleration ratio of a certain parallel algorithm is an ideal acceleration ratio, if the number of processors is doubled, the execution speed will also be doubled, that is, as ideal means, it has excellent scalability [17].

The value of efficiency E_p is generally between 0 and 1, and it is used to indicate how fully the processors involved in calculations are fully utilised when solving problems compared to the cost of communication and synchronisation. It is easy to see from the definition that the efficiency of an algorithm with a linear speedup and an algorithm executed on a single processor is 1.

Now let us calculate the computational efficiency and acceleration of different operation methods (table 1).

Table 1

Acceleration and efficiency of different computing solution

Time, T		Acceleration, $S_p = \frac{T_1}{T_p}$	Efficiency, $E_p = \frac{S_p}{p}$
Sequential calculation	Parallel calculation		
0.988 049	0.176 067	5.611 778	2.805 889

From the results in the last table, it is clear that $E_p > 1$, that is we obtain superlinear acceleration. In the process of parallel computing, sometimes there is a situation where the acceleration ratio is larger than the number of processors. The acceleration ratio obtained in this case is called a superlinear acceleration ratio [18].

The superlinear acceleration ratio has the following causes, such as the «cache effect» caused by the different storage levels of modern computers; specifically, compared with sequential computing, in parallel computing, not only are there more processors involved in calculations, caches from different processors are also pooled. In view of this, the cache of the collection is sufficient to provide the storage required for calculations. There is no need to use slower memory when executing the algorithm. Therefore, the memory reading time can be greatly reduced, what creates an additional acceleration effect for actual calculations.

Construction of models with order n

We have calculated and verified the motion status of 16 elements. Now when the number of elements increases exponentially to k (fig. 14), in another words it means we have the number of amount (20):

$$\mathrm{k} = 4^{\mathrm{n}} \left(\mathrm{n} = 1, 2, 3, \ldots\right). \tag{20}$$

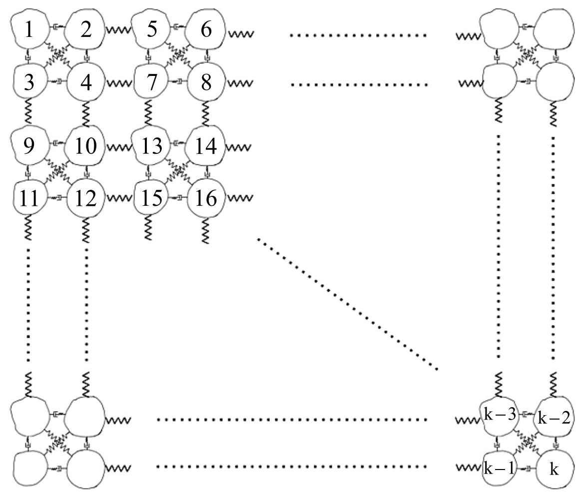

Fig. 14. The number of elements reaches to k

Using the second Lagrangian equation the kinetic energy (21) of the system is

$$T=\sum_{i=1}^{4}T_i=\frac{1}{2}m\dot{x}_1^2+\frac{1}{2}m\dot{x}_2^2+\ldots+\frac{1}{2}m\dot{x}_k^2. \tag{21}$$

With the potential energy of the system, the equation of motion of the entire system can be calculated by the formula (22):

$$\frac{d}{dt}\frac{\partial L}{\partial \dot{x}_i}-\frac{\partial L}{\partial x_i}=-\frac{\partial G}{\partial \dot{x}_i},\ i=\overline{1,\ \mathrm{k}}. \tag{22}$$

When the number of elements reaches k, we focus on two types of elements. The first type is the four elements in the corners, and the second type is the four elements in the center of the entire model.

In order, we first study the motion equations (table 2) of the four elements in the corners (fig. 15).

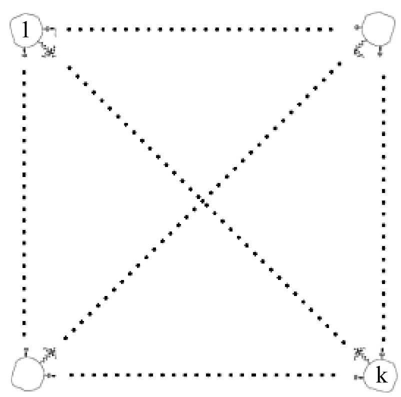

Fig. 15. The four elements in the corners

Table 2

Equation of motion for four elements in the corners

Location	The number of element	Equation of motion
Upper left corner	t = 1	$m\ddot{x}_1+k\left(\left(x_1+x_2\right)+\left(\left(l^2+\left(x_1-x_3\right)^2\right)^{\frac{1}{2}}-l\right)\left(l^2+\left(x_1-x_3\right)^2\right)^{-\frac{1}{2}}\left(x_1-x_3\right)-\right.$ $\left.-\left(\left(l^2+\left(l-x_1-x_4\right)^2\right)^{\frac{1}{2}}-l\right)\left(l^2+\left(l-x_1-x_4\right)^2\right)^{-\frac{1}{2}}\left(l-x_1-x_4\right)\right)=$ $=-\eta\left(\left(\dot{x}_1+\dot{x}_2\right)+\frac{\left(x_1-x_3\right)^2\left(\dot{x}_1-\dot{x}_3\right)}{l^2+\left(x_1-x_3\right)^2}\right)$

Ending of the table 2

Location	The number of element	Equation of motion
Upper right corner	$t = \frac{4}{3}\left(4^{n-1} - 1\right) + 2$ (n = 1, 2, 3, …)	$m\ddot{x}_t + k\left(\left(x_{t-1} + x_t\right) + \left(\left(l^2 + \left(x_t - x_{t+2}\right)^2\right)^{\frac{1}{2}} - l\right)\left(l^2 + \left(x_t - x_{t+2}\right)^2\right)^{-\frac{1}{2}}\left(x_t - x_{t+2}\right) - \left(\left(l^2 + \left(l - x_t - x_{t+1}\right)^2\right)^{\frac{1}{2}} - l\right)\left(l^2 + \left(l - x_t - x_{t+1}\right)^2\right)^{-\frac{1}{2}}\left(l - x_t - x_{t+1}\right)\right) = -\eta\left(\left(\dot{x}_{t-1} + \dot{x}_t\right) + \frac{\left(x_t - x_{t+2}\right)^2\left(\dot{x}_t - \dot{x}_{t+2}\right)}{l^2 + \left(x_t - x_{t+2}\right)^2}\right)$
Lower left corner	$t = \frac{8}{3}\left(4^{n-1} - 1\right) + 3$ (n = 1, 2, 3, …)	$m\ddot{x}_t + k\left(\left(x_t + x_{t+1}\right) - \left(\left(l^2 + \left(x_{t-2} - x_t\right)^2\right)^{\frac{1}{2}} - l\right)\left(l^2 + \left(x_{t-2} - x_t\right)^2\right)^{-\frac{1}{2}}\left(x_{t-2} - x_t\right) - \left(\left(l^2 + \left(l - x_{t-1} - x_t\right)^2\right)^{\frac{1}{2}} - l\right)\left(l^2 + \left(l - x_{t-1} - x_t\right)^2\right)^{-\frac{1}{2}}\left(l - x_{t-1} - x_t\right)\right) = -\eta\left(\left(\dot{x}_t + \dot{x}_{t+1}\right) - \frac{\left(x_{t-2} - x_t\right)^2\left(\dot{x}_{t-2} - \dot{x}_t\right)}{l^2 + \left(x_{t-2} - x_t\right)^2}\right)$
Lower right corner	$t = 4^n$ (n = 1, 2, 3, …)	$m\ddot{x}_t + k\left(\left(x_{t-1} + x_t\right) - \left(\left(l^2 + \left(x_{t-2} - x_t\right)^2\right)^{\frac{1}{2}} - l\right)\left(l^2 + \left(x_{t-2} - x_t\right)^2\right)^{-\frac{1}{2}}\left(x_{t-2} - x_t\right) - \left(\left(l^2 + \left(l - x_{t-3} - x_t\right)^2\right)^{\frac{1}{2}} - l\right)\left(l^2 + \left(l - x_{t-3} - x_t\right)^2\right)^{-\frac{1}{2}}\left(l - x_{t-3} - x_t\right)\right) = -\eta\left(\left(\dot{x}_{t-1} + \dot{x}_t\right) - \frac{\left(x_{t-2} - x_t\right)^2\left(\dot{x}_{t-2} - \dot{x}_t\right)}{l^2 + \left(x_{t-2} - x_t\right)^2}\right)$

Then we study the motion equations (table 3) of the four elements in the center of the system which are shown in fig. 16.

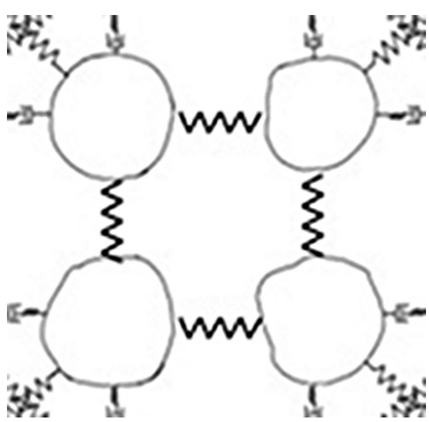

Fig. 16. The four elements in the center

Table 3

Equation of motion for four elements in the center

Location	The number of element	Equation of motion
Upper left	$t = 4^n - 1$ (n = 2, 3, 4, …)	$m\ddot{x}_t + k\left(\left(x_{t-1} + x_t\right) - \left(\left(l^2 + \left(x_{t-2} - x_t\right)^2\right)^{\frac{1}{2}} - l\right)\left(l^2 + \left(x_{t-2} - x_t\right)^2\right)^{-\frac{1}{2}}\left(x_{t-2} - x_t\right) - \left(\left(l^2 + \left(l - x_{t-3} - x_t\right)^2\right)^{\frac{1}{2}} - l\right)\left(l^2 + \left(l - x_{t-3} - x_t\right)^2\right)^{-\frac{1}{2}}\left(l - x_{t-3} - x_t\right)\right) = -\eta\left(\left(\dot{x}_{t-1} + \dot{x}_t\right) - \frac{\left(x_{t-2} - x_t\right)^2\left(\dot{x}_{t-2} - \dot{x}_t\right)}{l^2 + \left(x_{t-2} - x_t\right)^2}\right)$
Upper right	$t = \frac{20}{3}\left(4^{n-2} - 1\right) + 7$ (n = 2, 3, 4, …)	$m\ddot{x}_t + k\left(\left(x_t + x_{t+1}\right) - \left(\left(l^2 + \left(x_{t-2} - x_t\right)^2\right)^{\frac{1}{2}} - l\right)\left(l^2 + \left(x_{t-2} - x_t\right)^2\right)^{-\frac{1}{2}}\left(x_{t-2} - x_t\right) + \left(\left(l^2 + \left(x_t - x_{\frac{9}{5}t + \frac{2}{5}}\right)^2\right)^{\frac{1}{2}} - l\right)\left(l^2 + \left(x_t - x_{\frac{9}{5}t + \frac{2}{5}}\right)^2\right)^{-\frac{1}{2}}\left(x_t - x_{\frac{9}{5}t + \frac{2}{5}}\right) - \left(\left(l^2 + \left(l - x_{t-1} - x_t\right)^2\right)^{\frac{1}{2}} - l\right)\left(l^2 + \left(l - x_{t-1} - x_t\right)^2\right)^{-\frac{1}{2}}\left(l - x_{t-1} - x_t\right) + \left(x_{\frac{3}{5}t - \frac{1}{5}} + x_t\right)\right) = -\eta\left(\left(\dot{x}_t + \dot{x}_{t+1}\right) - \frac{\left(x_{t-2} - x_t\right)^2\left(\dot{x}_{t-2} - \dot{x}_t\right)}{l^2 + \left(x_{t-2} - x_t\right)^2}\right)$
Lower left	$t = \frac{28}{3}\left(4^{n-2} - 1\right) + 10$ (n = 2, 3, 4, …)	$m\ddot{x}_t + k\left(\left(x_{t-1} + x_t\right) + \left(\left(l^2 + \left(x_t - x_{t+2}\right)^2\right)^{\frac{1}{2}} - l\right)\left(l^2 + \left(x_t - x_{t+2}\right)^2\right)^{-\frac{1}{2}}\left(x_t - x_{t+2}\right) - \left(\left(l^2 + \left(x_{\frac{3}{7}t - \frac{2}{7}} - x_t\right)^2\right)^{\frac{1}{2}} - l\right)\left(l^2 + \left(x_{\frac{3}{7}t - \frac{2}{7}} - x_t\right)^2\right)^{-\frac{1}{2}}\left(x_{\frac{3}{7}t - \frac{2}{7}} - x_t\right) - \left(\left(l^2 + \left(l - x_t - x_{t+1}\right)^2\right)^{\frac{1}{2}} - l\right)\left(l^2 + \left(l - x_t - x_{t+1}\right)^2\right)^{-\frac{1}{2}}\left(l - x_t - x_{t+1}\right) + \left(x_t + x_{\frac{9}{7}t + \frac{1}{7}}\right)\right) = -\eta\left(\left(\dot{x}_{t-1} + \dot{x}_t\right) + \frac{\left(x_t - x_{t+2}\right)^2\left(\dot{x}_t - \dot{x}_{t+2}\right)}{l^2 + \left(x_t - x_{t+2}\right)^2}\right)$

Ending of the table 3

Location	The number of element	Equation of motion
Lower right	$t = \frac{8}{3}\left(4^{n-1} - 1\right) + 3$ (n = 2, 3, 4, …)	$m\ddot{x}_t + k\Bigg(\left(x_{t-1} + x_t\right) + \Big(\left(l^2 + \left(x_t - x_{t+2}\right)^2\right)^{\frac{1}{2}} - l\Big)\left(l^2 + \left(x_t - x_{t+2}\right)^2\right)^{-\frac{1}{2}}\left(x_t - x_{t+2}\right) - \Big(\Big(l^2 + \Big(x_{\frac{5}{9}t - \frac{2}{9}} - x_t\Big)^2\Big)^{\frac{1}{2}} - l\Big)\Big(l^2 + \Big(x_{\frac{5}{9}t - \frac{2}{9}} - x_t\Big)^2\Big)^{-\frac{1}{2}}\Big(x_{\frac{5}{9}t - \frac{2}{9}} - x_t\Big) - \Big(\left(l^2 + \left(l - x_t - x_{t+3}\right)^2\right)^{\frac{1}{2}} - l\Big)\left(l^2 + \left(l - x_t - x_{t+3}\right)^2\right)^{-\frac{1}{2}}\left(l - x_t - x_{t+3}\right) + \Big(x_{\frac{7}{9}t - \frac{1}{9}} + x_t\Big)\Bigg) = -\eta\left(\left(\dot{x}_t + \dot{x}_{t+1}\right) + \frac{\left(x_t - x_{t+2}\right)^2\left(\dot{x}_t - \dot{x}_{t+2}\right)}{l^2 + \left(x_t - x_{t+2}\right)^2}\right)$

Simulation when system consists of 64 elements. We have studied the situation when there are 4 (n = 1) and 16 (n = 2) elements. Now we calculate and verify the motion state of the system when n = 3, 4, 5, and simulate the four elements in the center of the system.

When n = 3, then the total number of amount is k = 64 (fig. 17).

In order, we calculate the Lagrangian equations of motion for the four elements in the center (fig. 18, table 4).

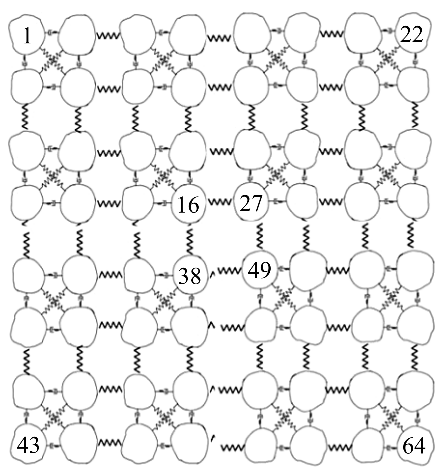

Fig. 17. The system when n = 3

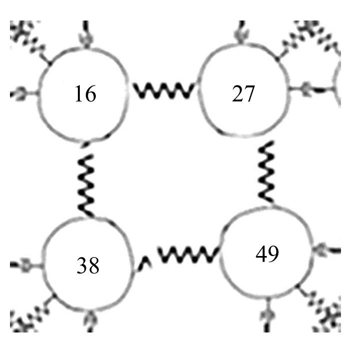

Fig. 18. The four elements in the center of the system when there are totally 64 elements

Table 4

Equation of motion for four elements in the center when n = 3

Location	The number of element	Equation of motion
Upper left	t = 16	$$m\ddot{x}_{16} + k\left((x_{15}+x_{16}) - \left(\left(l^2+(x_{14}-x_{16})^2\right)^{\frac{1}{2}} - l\right)\left(l^2+(x_{14}-x_{16})^2\right)^{-\frac{1}{2}}(x_{14}-x_{16}) - - \left(\left(l^2+(l-x_{13}-x_{16})^2\right)^{\frac{1}{2}} - l\right)\left(l^2+(l-x_{13}-x_{16})^2\right)^{-\frac{1}{2}}(l-x_{13}-x_{16})\right) = = -\eta\left((\dot{x}_{15}+\dot{x}_{16}) - \frac{(x_{14}-x_{16})^2(\dot{x}_{14}-\dot{x}_{16})}{l^2+(x_{14}-x_{16})^2}\right)$$
Upper right	t = 27	$$m\ddot{x}_{27} + k\left((x_{27}+x_{28}) - \left(\left(l^2+(x_{25}-x_{27})^2\right)^{\frac{1}{2}} - l\right)\left(l^2+(x_{25}-x_{27})^2\right)^{-\frac{1}{2}}(x_{25}-x_{27}) + + \left(\left(l^2+(x_{27}-x_{49})^2\right)^{\frac{1}{2}} - l\right)\left(l^2+(x_{27}-x_{49})^2\right)^{-\frac{1}{2}}(x_{27}-x_{49}) - - \left(\left(l^2+(l-x_{26}-x_{27})^2\right)^{\frac{1}{2}} - l\right)\left(l^2+(l-x_{26}-x_{27})^2\right)^{-\frac{1}{2}}(l-x_{26}-x_{27}) + (x_{16}+x_{27})\right) = = -\eta\left((\dot{x}_{27}+\dot{x}_{28}) - \frac{(x_{25}-x_{27})^2(\dot{x}_{25}-\dot{x}_{27})}{l^2+(x_{25}-x_{27})^2}\right)$$
Lower left	t = 38	$$m\ddot{x}_{38} + k\left((x_{37}+x_{38}) + \left(\left(l^2+(x_{38}-x_{40})^2\right)^{\frac{1}{2}} - l\right)\left(l^2+(x_{38}-x_{40})^2\right)^{-\frac{1}{2}}(x_{38}-x_{40}) - - \left(\left(l^2+(x_{16}-x_{38})^2\right)^{\frac{1}{2}} - l\right)\left(l^2+(x_{16}-x_{38})^2\right)^{-\frac{1}{2}}(x_{16}-x_{38}) - - \left(\left(l^2+(l-x_{38}-x_{39})^2\right)^{\frac{1}{2}} - l\right)\left(l^2+(l-x_{38}-x_{39})^2\right)^{-\frac{1}{2}}(l-x_{38}-x_{39}) + (x_{38}+x_{49})\right) = = -\eta\left((\dot{x}_{37}+\dot{x}_{38}) + \frac{(x_{38}-x_{40})^2(\dot{x}_{38}-\dot{x}_{40})}{l^2+(x_{38}-x_{40})^2}\right)$$
Lower right	t = 49	$$m\ddot{x}_{49} + k\left((x_{49}+x_{50}) + \left(\left(l^2+(x_{49}-x_{51})^2\right)^{\frac{1}{2}} - l\right)\left(l^2+(x_{49}-x_{51})^2\right)^{-\frac{1}{2}}(x_{49}-x_{51}) - - \left(\left(l^2+(x_{27}-x_{49})^2\right)^{\frac{1}{2}} - l\right)\left(l^2+(x_{27}-x_{49})^2\right)^{-\frac{1}{2}}(x_{27}-x_{49}) - - \left(\left(l^2+(l-x_{49}-x_{52})^2\right)^{\frac{1}{2}} - l\right)\left(l^2+(l-x_{49}-x_{52})^2\right)^{-\frac{1}{2}}(l-x_{49}-x_{52}) + (x_{38}+x_{49})\right) = = -\eta\left((\dot{x}_{49}+\dot{x}_{50}) + \frac{(x_{49}-x_{51})^2(\dot{x}_{49}-\dot{x}_{51})}{l^2+(x_{49}-x_{51})^2}\right)$$

Then we simulate the motion image of the four elements in the center of the system. The initial boundary conditions are displacement, velocity and impulse as in the previous task.

Initial condition (displacement). For the variant where the initial condition is displacement, we reduce the displacement from 0.5 to 0.05 m and finally reduce it to 0.005 m, in order to study the difference in the motion of the model (table 5).

Table 5

The movement of the four elements in the center under different initial displacement with total of 64 elements

The parameters and the initial conditions are $m = 2$ kg, $l = 0.1$ m, $k = 100$ N/m, $c = 0.5$ N · s/m, $t = 10$ s, $x_1 = 0.5$ m										
$t = 0$ s	$t = 1$ s	$t = 2$ s	$t = 3$ s	$t = 4$ s	$t = 5$ s	$t = 6$ s	$t = 7$ s	$t = 8$ s	$t = 9$ s	$t = 10$ s
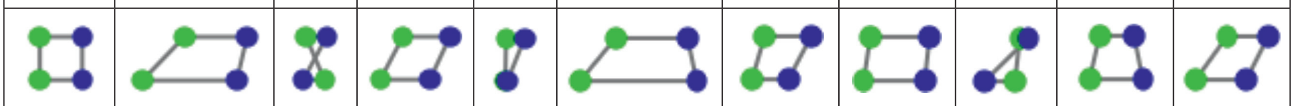										
The parameters and the initial conditions are $m = 2$ kg, $l = 0.1$ m, $k = 100$ N/m, $c = 0.5$ N · s/m, $t = 10$ s, $x_1 = 0.05$ m										
$t = 0$ s	$t = 1$ s	$t = 2$ s	$t = 3$ s	$t = 4$ s	$t = 5$ s	$t = 6$ s	$t = 7$ s	$t = 8$ s	$t = 9$ s	$t = 10$ s
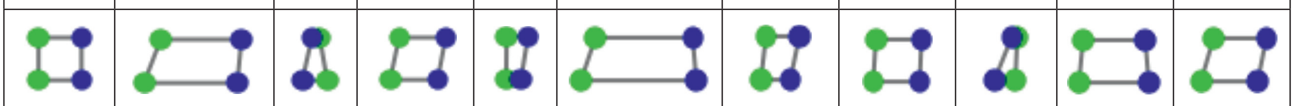										
The parameters and the initial conditions are $m = 2$ kg, $l = 0.1$ m, $k = 100$ N/m, $c = 0.5$ N · s/m, $t = 10$ s, $x_1 = 0.005$ m										
$t = 0$ s	$t = 1$ s	$t = 2$ s	$t = 3$ s	$t = 4$ s	$t = 5$ s	$t = 6$ s	$t = 7$ s	$t = 8$ s	$t = 9$ s	$t = 10$ s
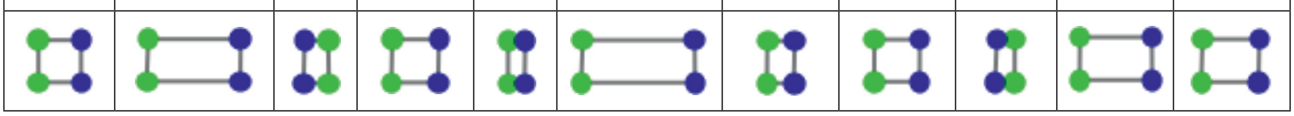										

Initial condition (velocity). The parameters and the initial conditions are

$$m = 2 \text{ kg}, l = 0.1 \text{ m}, k = 100 \text{ N/m}, c = 0.5 \text{ N} \cdot \text{s/m}, t = 10 \text{ s}.$$

There is an initial velocity in the horizontal direction to any element which is shown in fig. 19, and in this variant the initial velocity is $v_1 = 0.5$ m/s.

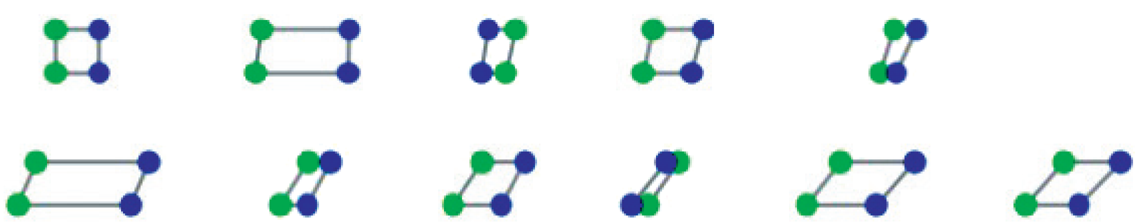

Fig. 19. The movement of the four elements in the center under the initial velocity with total of 64 elements

Initial condition (impulse). The parameters and the initial conditions are

$$m = 2 \text{ kg}, l = 0.1 \text{ m}, k = 100 \text{ N/m}, c = 0.5 \text{ N} \cdot \text{s/m}, t = 10 \text{ s}.$$

There is an initial impulse in the horizontal direction to any element which is shown in fig. 20, and in this variant the initial impulse with the function is the same as in the previous study.

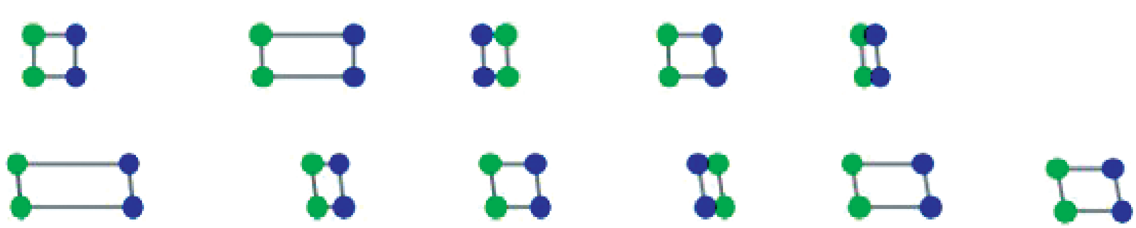

Fig. 20. The movement of the four elements in the center under initial impulse with total of 64 elements

Simulation when the system consists of 256 elements. When n = 4, then the number of amount is k = 256 (fig. 21).

As what we did in the previous study then we also simulate the motion image of the four elements in the center of the system (fig. 22). The initial boundary conditions are displacement, velocity and impulse as in the previous task (table 6).

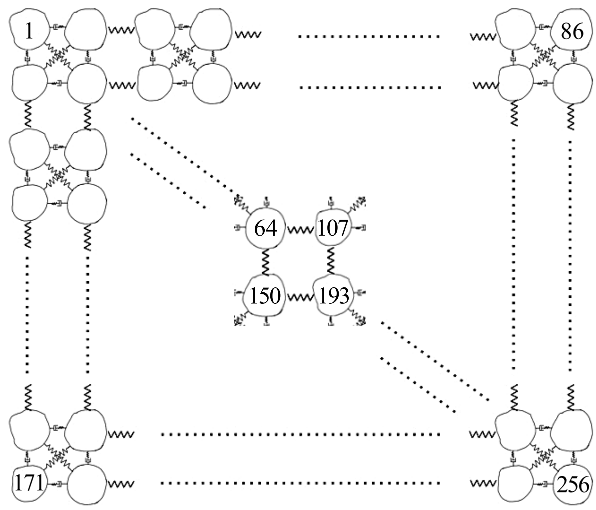

Fig. 21. The system when n = 4

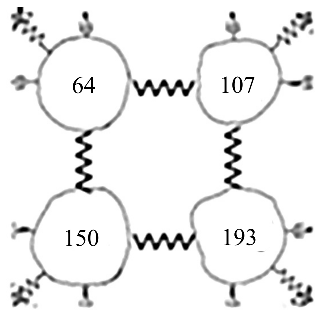

Fig. 22. The four elements in the center of the system when there are totally 256 elements

Table 6

The simulation of four elements in the center of the system which contains 256 elements under the different initial conditions

Initial condition (displacement): $m = 2$ kg, $l = 0.1$ m, $k = 100$ N/m, $c = 0.5$ N · s/m, $t = 10$ s, $x_1 = 0.5$ m
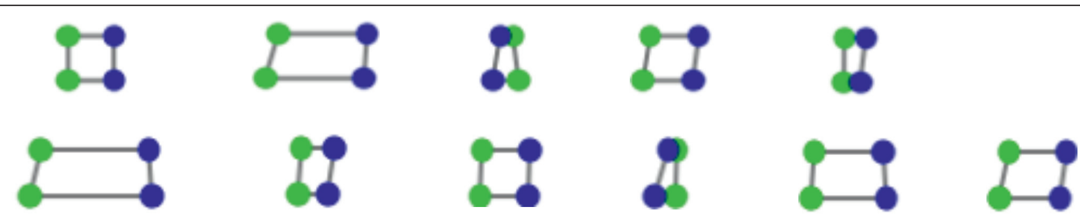
Initial condition (velocity): $m = 2$ kg, $l = 0.1$ m, $k = 100$ N/m, $c = 0.5$ N · s/m, $t = 10$ s, $v_1 = 0.5$ m/s
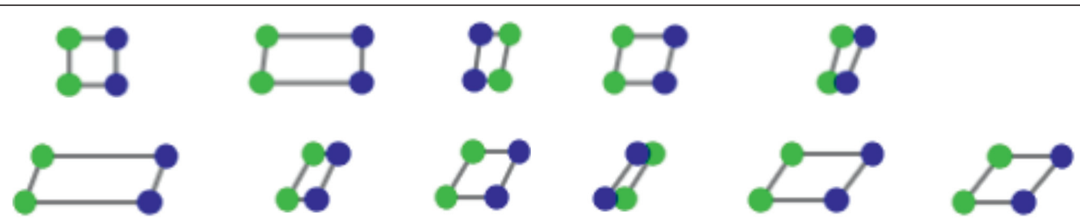
Initial condition (impulse): $m = 2$ kg, $l = 0.1$ m, $k = 100$ N/m, $c = 0.5$ N · s/m, $t = 10$ s, the impulse is the same as previous task
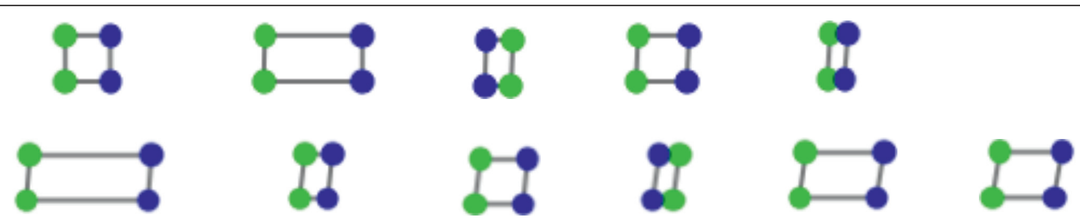

Simulation when the system consists of 256 elements. When n = 5, then the number of amount is k = 1024 (fig. 23).

We already study the situation when n = 3 and n = 4. As what we did in the previous study then we also simulate the motion image of the four elements in the center of the system (fig. 24). The initial boundary conditions are displacement, velocity and impulse as in the previous task (table 7).

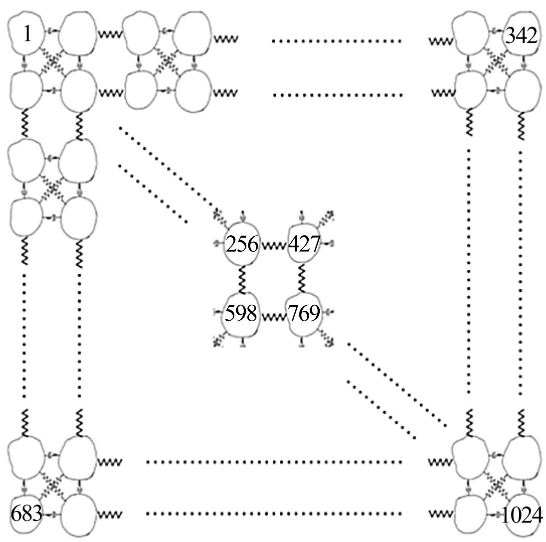

Fig. 23. The system when n = 5

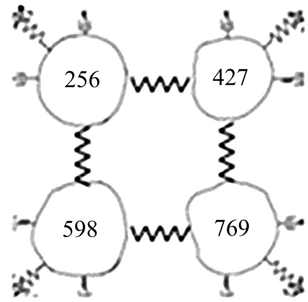

Fig. 24. The four elements in the center of the system when there are totally 1024 elements

Table 7

The simulation of four elements in the center of system which contains 1024 elements under the different initial conditions

Initial condition (displacement): $m = 2$ kg, $l = 0.1$ m, $k = 100$ N/m, $c = 0.5$ N · s/m, $t = 10$ s, $x_1 = 0.5$ m
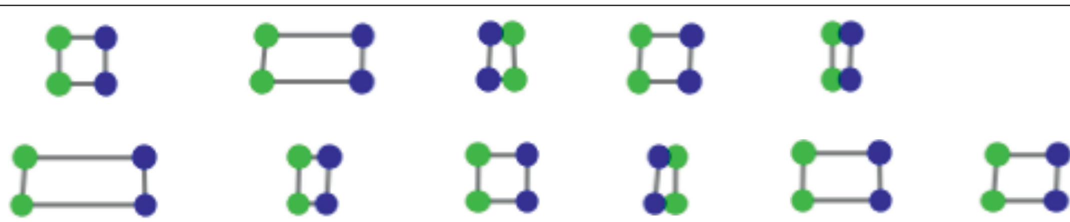
Initial condition (velocity): $m = 2$ kg, $l = 0.1$ m, $k = 100$ N/m, $c = 0.5$ N · s/m, $t = 10$ s, $v_1 = 0.5$ m/s
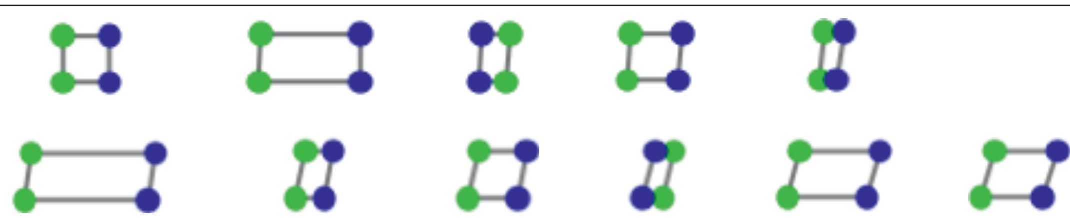
Initial condition (impulse): $m = 2$ kg, $l = 0.1$ m, $k = 100$ N/m, $c = 0.5$ N · s/m, $t = 10$ s, the impulse is the same as in the previous task
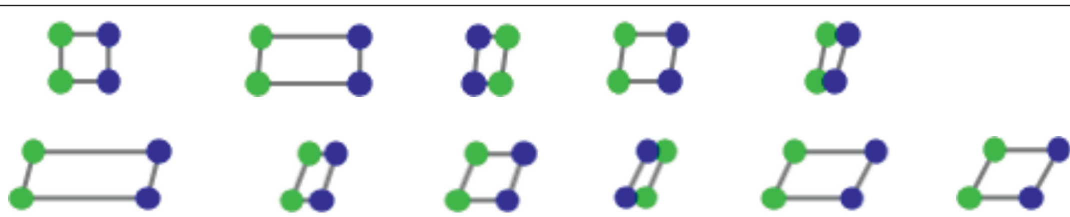

Conclusions

This article introduces the application of numerical simulation methods in geomechanical engineering problems, relevant principles and lists specific situations under different boundary conditions. Finally, it points out the development directions and problems that still exist in current numerical simulation experiments. The research proposes a block element that can take into account its deformation capability under external loads. Based on this type of block element, it seems promising to simulate the SSS of the rock mass region through the discrete element method, since considering the rock mass region within the framework of the continuum model is a rather «rough» approximation assumption. Another important fact is that the introduced block elements can be used to study problems under static as well as dynamic loads.

For real geological and rock soil mechanics problems, the solution proposed in this article can be used as a basic model construction method. In order to further improve the accuracy and practicality of the solution, this can be achieved by changing the structure and size of the block units, as well as the density and connection methods of various link keys between units. Developing codes that compute faster and more accurate models is a direction for future research. With the increasing scale of geomechanical engineering, our requirements for the level of scientific research and the accuracy of solutions in engineering construction are getting higher and higher. That is the reason numerical simulation methods have become an effective solution. Numerical simulation is of great significance for understanding the SSS and movement change of rock and soil blocks in geomechanical engineering. It can also provide theoretical basis for actual engineering and play a role in safety protection.

References

1. Belytschko T, Krongauz Y, Organ D, Fleming M, Krysl P. Meshless methods: an overview and recent developments. *Computer Methods in Applied Mechanics and Engineering*. 1996;139(1–4):3–47. DOI: 10.1016/S0045-7825(96)01078-X.

2. Li SH, Zhao MH, Wang YN, Wang JG. A continuum-based discrete element method for continuous deformation and failure process. In: Forschungsbereich Struktursimulation und Ingenieurholzbau. *6th World Congress on Computational Mechanics (WCCM VI) in conjunction with the 2nd Asian-Pacific Congress on Computational Mechanics (APCOM'04); 2004 September 5–10; Beijing, China*. Beijing: Tsinghua University Press; 2004. 5 p.

3. Ariffin AK, Huzni S, Nor MJM, Mohamed NAK. Hybrid finite-discrete element simulation of crack propagation under mixed mode loading condition. *Key Engineering Materials*. 2006;306–308:495–500. DOI: 10.4028/www.scientific.net/KEM.306-308.495.

4. Karami A, Stead D. Asperity degradation and damage in the direct shear test: a hybrid FEM/DEM approach. *Rock Mechanics and Rock Engineering*. 2008;41(2):229–266. DOI: 10.1007/s00603-007-0139-6.

5. Morris JP, Rubin MB, Block GI, Bonner MP. Simulations of fracture and fragmentation of geologic materials using combined FEM/DEM analysis. *International Journal of Impact Engineering*. 2006;33(1–12):463–473. DOI: 10.1016/j.ijimpeng.2006.09.006.

6. Zhurkina DS, Klishin SV, Lavrikov SV, Leonov MG. DEM-based modeling of shear localization and transition of geomedium to unstable deformation. *Fiziko-tekhnicheskie problemy razrabotki poleznykh iskopaemykh*. 2022;3:13–22. Russian. DOI: 10.15372/FTPRPI20220302.

7. Jiang M, Yu H-S. Application of discrete element method to geomechanics. In: Wu W, Yu H-S, editors. *Modern trends in geomechanics*. Berlin: Springer; 2006. p. 241–269 (Springer proceedings in physics; volume 106).

8. Chigarev AV, Botogova MG, Mikhasev GI. Propagation of a surface wave near a randomly rough surface. *Journal of the Belarusian State University. Mathematics and Informatics*. 2023;1:38–48. Russian.

9. Chanyshev AI, Abdulin IM. New formulations of geomechanical problems with regard to post-limit deformation of rocks. *Fiziko-tekhnicheskie problemy razrabotki poleznykh iskopaemykh*. 2022;5:12–27. DOI: 10.15372/FTPRPI20220502.

10. Zhuravkov M, Shunying J, Kanavalau A. Modeling of deformation processes in rock massif in the vicinity of underground goafs considering the formation of discontinuity zones. *Theoretical and Applied Mechanics Letters*. 2020;10(2):92–97. DOI: 10.1016/j.taml.2020.01.012.

11. Shi G-H. *Discontinuous deformation analysis: a new numerical model for the statics and dynamics of block systems* [dissertation]. Berkeley: University of California; 1988. 378 p.

12. Zhuravkov MA, Starovoitov EI. *Matematicheskie modeli mekhaniki tverdykh tel* [Mathematical models of solid state mechanics]. Minsk: Belarusian State University; 2021. 535 p. Russian.

13. Boyce WE, DiPrima RC. *Elementary differential equations and boundary value problems*. New York: John Wiley and Sons; 1995. 485 p.

14. Sansour C, Skatulla S. A strain gradient generalized continuum approach for modelling elastic scale effects. *Computer Methods in Applied Mechanics and Engineering*. 2009;198(15–16):1401–1412. DOI: 10.1016/j.cma.2008.12.031.

15. Stewart J. *Calculus*. 3rd edition. Pacific Grove: Brooks Cole; 1995. 112 p.

16. Aggarwal A, Chazelle B, Guibas L, O'Dunlaing C, Yap C. Parallel computational geometry. *Algorithmica*. 1988;3(3):293–327.

17. Atallah MJ, Goodrich MT. Efficient parallel solutions to some geometric problems. *Journal of Parallel and Distributed Computing*. 1986;3(4):492–507. DOI: 10.1016/0743-7315(86)90011-0.

18. Kumar V, Grama A, Gupta A, Karypis G. *Introduction to parallel computing: design and analysis of algorithms*. Redwood City: Benjamin Cummings; 1994. 600 p.

Received 30.05.2024 / revised 22.10.2024 / accepted 22.10.2024.